Mineralogy and Petrology (2007) 90: 249–270
DOI 10.1007/s00710-006-0176-y
Printed in The Netherlands

Mineralogy and Petrology

Re–Os molybdenite and Ar–Ar phlogopite dating of Cu–Fe–Au–Mo (W) deposits in southeastern Hubei, China

G.-Q. Xie[1,2,3], **J.-W. Mao**[2], **R.-L. Li**[3], **W.-J. Qü**[4], **F. Pirajno**[5], and **A.-D. Du**[4]

[1] State Key Laboratory of Geological Process and Mineral Recourse, China University of Geosciences, Beijing, China
[2] Institute of Mineral Resources, Chinese Academy of Geological Sciences, Beijing, China
[3] State Key Laboratory of Ore Deposit Geochemistry, Institute of Geochemistry, Chinese Academy of Sciences, Guiyang, China
[4] National Research Centers of Geoanalysis, Chinese Academy of Geological Sciences, Beijing, China
[5] Geological Survey of Western Australia, 100 Plain Street, Perth, WA, Australia

Received May 5, 2006; accepted November 15, 2006
Published online March 13, 2007;
Editorial handling: J. G. Raith

Summary

The Cu–Fe–Au–Mo (W) deposits in southeastern Hubei are an important component of the Middle–Lower Yangtze River metallogenic belt. Molybdenite from the Fengshandong Cu- (Mo), Ruanjiawan W–Cu- (Mo), Qianjiawan Cu–Au, Tongshankou Cu–Mo and Tonglüshan Cu- (Fe) deposits yielded Re–Os ages of 144.0 ± 2.1 Ma, 143.6 ± 1.7 Ma, 137.7 ± 1.7 Ma, 142.3 ± 1.8–143.7 ± 1.8 Ma and 137.8 ± 1.7–138.1 ± 1.8 Ma, respectively. Phlogopite from the Tieshan Fe- (Cu) deposit yielded an Ar–Ar age of 140.9 ± 1.2 Ma. These data and other published isotopic ages (Re–Os molybdenite and Ar–Ar mica ages) for the Cu–Fe–Au–Mo (W) deposits in the Middle–Lower Yangtze River metallogenic belt show that Cu–Fe–Au–Mo (W) mineralisation in the Tongling, Anqing, Jiurui and Edong ore districts developed in a narrow time span between 135.5 and 144.9 Ma, reflecting an important regional metallogenic event. An integrated study of available petrological and geochronological data, together with relationships to magmatism and the regional geodynamic framework, indicate that the Cu–Fe–Au–Mo (W) mineralisation in the Middle–Lower Yangtze River belt occurred during a regime of lithospheric extension. This extension is probably related to Late Mesozoic processes of lower crustal delamination and lithospheric thinning in East China.

Introduction

The Middle–Lower Yangtze River belt, an area of ~30,000 km^2, extending ~450 km from southeastern Hubei eastward to Jiangsu province, is one of the most important mineral provinces in East China. The southeastern Hubei region is one of the important areas in the Middle–Lower Yangtze River metallogenic belt, comprising the Edong ore district and the western part of the Jiurui ore district, where more than 50 Cu–Fe–Au–Mo (W) deposits have been discovered so far. The main types of ore systems include Fe–Cu skarn, Cu–Au–Mo- (W) porphyry, skarn and stratabound deposits, all of which are spatially associated with Late Mesozoic granitoids (e.g. *Pan* and *Dong*, 1999; *Mao* et al., 2006a). However, the ages of the granodiorite porphyry, diorite and granodiorite that are associated with these mineral systems are poorly constrained by K–Ar and Rb–Sr isochron methods, and range from 205 to 90 Ma (e.g. *Zhou* and *Ren*, 1994; *Zhai* et al., 1996; *Pan* and *Dong*, 1999). Consequently, there is no direct and precise geochronology for ore formation. Re–Os and Ar–Ar isotopic systems are particularly suitable to precisely constrain the ages of the mineralisation and the related hydrothermal altered rocks. Here we present new Re–Os molybdenite and Ar–Ar phlogopite ages for some Cu–Fe–Au–Mo- (W) deposits to constrain the timing and duration of mineralisation in southeastern Hubei. These data and the previously published isotopic ages for other Cu–Fe–Au deposits and related rocks are evaluated to constrain the timing and geodynamic setting of the mineralisation in the Middle–Lower Yangtze River metallogenic belt.

Geological setting

The Middle–Lower Yangtze River metallogenic belt is located on the northern margin of the Yangtze Block and in the southeast of the North China Block and Dabieshan orogenic belt (Fig. 1). This belt is bounded by the Xiangfan-Guangji fault (XGF) to the northwest, the Tangcheng-Lijiang regional strike-slip fault (TLF) to the northeast, and the Yangxing-Changzhou fault (YCF) to the south (Fig. 1). The basement rocks comprise metamorphic biotite-hornblende gneisses, a trondjhemite–tonalite–granodiorite suite (TTG), and supracrustal rocks of 2900–990 Ma (e.g. *Chang* et al., 1991; *Zhai* et al., 1992). Unconformably overlying the metamorphic basement is a thick succession comprising Sinian clastic, carbonate and chert, Cambrian chert nodule, mudstone and argillaceous limestone, Ordovician limestone and dolomitic limestone, Silurian clastic rocks, Devonian sandstone, Carboniferous sandstone, siltstone and limestone, Permian shale and limestone, and Triassic argillaceous clastic rocks (*Chang* et al., 1991; *Zhai* et al., 1992). Intrusive magmatism and volcanism occurred in the Late Jurassic–Early Cretaceous along the Middle–Lower Yangtze River metallogenic belt.

In this metallogenic belt Late Mesozoic magmatism mainly consists of Late Jurassic to Cretaceous calc-alkaline intrusive rocks and Early Cretaceous sub-alkaline to alkaline volcanic rocks (*Pei* and *Hong*, 1995; *Chen* et al., 2001; *Xie* et al., 2006). These igneous rocks are divided into: 1) calc-alkaline granodiorite series, and 2) Na-rich calc-alkaline diorite series. The former consists of gabbro, diorite, quartz diorite and granodiorite classified as I-type, and are related to Cu–

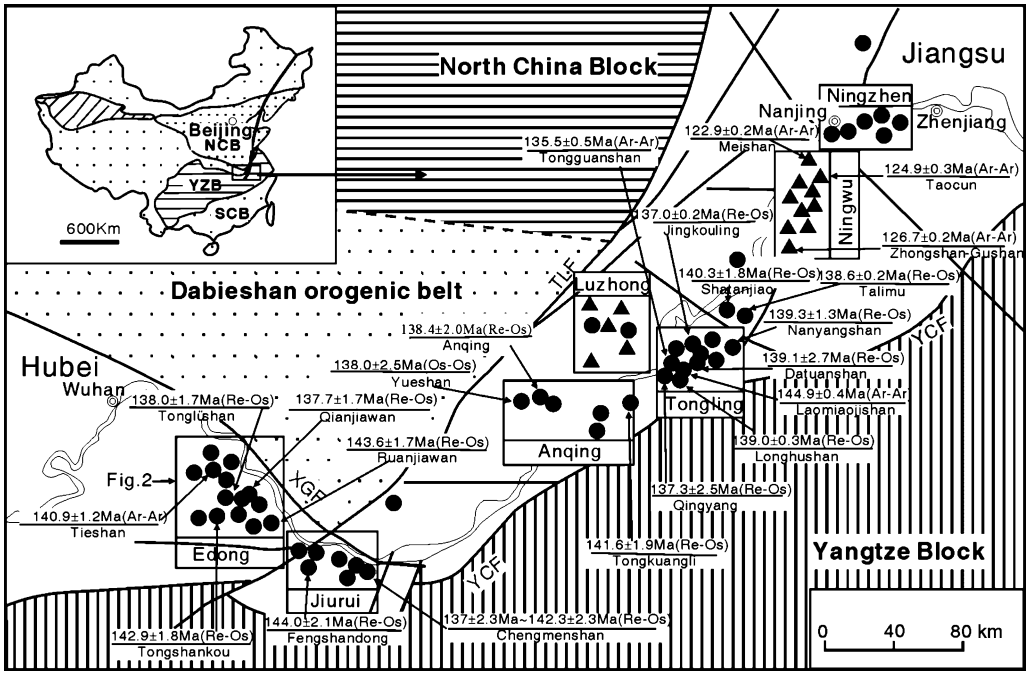

Fig. 1. Distribution of Cu–Fe–Au–Mo deposits in the Middle–Lower Yangtze River metallogenic belt (modified from *Pan* and *Dong*, 1999), showing the mineralisation ages of the Tongshankou, Tonglüshan, Qianjiawan, Ruanjiawan, Tieshan and Fengshandong deposits (this study), the Chengmengshan deposit (*Wu* and *Zou*, 1997; *Mao* et al., 2006a), the Anqing, Tukuangli, Shantanjiao, Nanyanshan and Datuanshan deposits (*Mao* et al., 2006a), the Yueshan and Qingyang deposits (*Sun* et al., 2003), the Jingkouling, Tongguanshan and Laomiaojishan deposits (*Meng* et al., 2004) and the Talimu deposit (*Zeng* et al., 2004). *NCB* North China Block; *SCB* South China Block; *YZB* Yangtze Block; ●: Porphyry, skarn and stratabound Cu–Fe–Au–Mo- (W) deposits; ▲: Magnetite porphyry deposit; *XGF* Xiangfan-Guangji Fault; *TLF* Tangcheng-Lijiang Fault; *YCF* Yangxing-Changzhou Fault

Fe–Au–Mo mineralisation; they were formed by crust–mantle interaction during a tectonic regime of extension and collapse (*Pei* and *Hong*, 1995). The Na-rich series is composed of pyroxene diorite porphyry, diorite porphyry and their eruptive equivalents (basalt–andesite–rhyolite), they are associated with skarn and magnetite porphyry deposits in ore districts, such as the Ningwu basin (*Ningwu Research Group*, 1978). Recently, precise ages (i.e. U–Pb zircon SHRIMP and LA-ICPMS) indicate that the granite–granodiorite–diorite suite was emplaced between 152 and 121 Ma and that the basalt–andesite–rhyolite suite was erupted at 127–131 Ma (e.g. *Xie* et al., 2005, 2006).

The southeastern Hubei area is situated in the western part of the Middle–Lower Yangtze River metallogenic belt (Figs. 1, 2). In this area Sinian to Middle Jurassic shallow-marine carbonate rocks, clastic rocks, and flysch successions are widespread. The host rocks to the mineralisation are dominantly limestone and dolomite of the Lower Triassic Daye Formation. Late Jurassic–Cretaceous volcanic and sedimentary rocks outcrop in the western part of the ore district, where

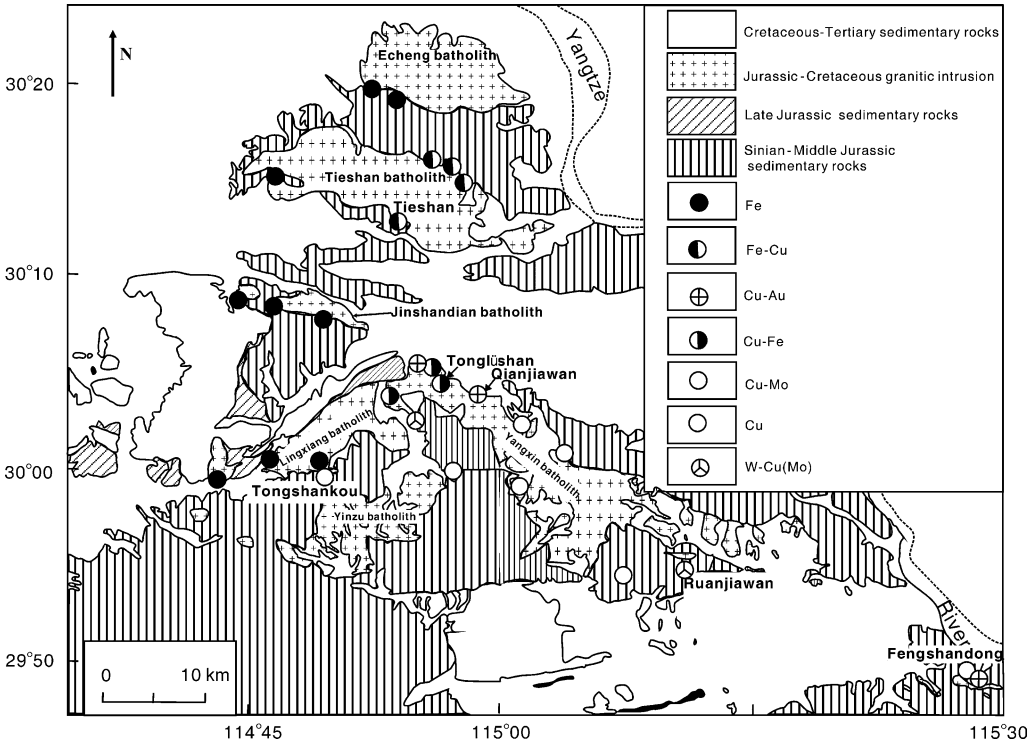

Fig. 2. Simplified geological map of southeastern Hubei, showing distribution of Late Mesozoic Cu–Fe–Au–Mo- (W) deposits (modified from *Shu* et al., 1992)

voluminously rhyolites and andesite, and minor basalts are present (*Chang* et al., 1991; *Zhai* et al., 1992; *Xie* et al., 2006) (Fig. 2).

In southeastern Hubei Late Mesozoic granitoid plutons and granodiorite porphyry stocks occupy approximately 17% of the area (*Pan* and *Dong*, 1999). As shown in Fig. 2, they include six complex granitoid batholiths, comprising the Echeng granite and quartz diorite (94–126 Ma, K–Ar age), Tieshan granodiorite and diorite (164 Ma, zircon U–Pb age; 120–150 Ma, K–Ar age), and monzonite (133.4 Ma, Ar–Ar age), Jinshandian quartz monzonite and granite (94–142 Ma, K–Ar age), Lingxiang diorite (101–145 Ma, whole rock and biotite K–Ar age; 145–157 Ma, Rb–Sr isochron age), Yinzu quartz diorite (150–189 Ma, biotite K–Ar age), and Yangxin granodiorite and diorite (*Shu* et al., 1992; *Zhou* and *Ren*, 1994; *Pan* and *Dong*, 1999). In addition, several small granodiorite porphyry stocks i.e. Tongshankou, Ruanjiawan, Fengshandong, are genetically related to Cu–Mo- (W) mineralisation (Fig. 2). Though the emplacement ages of the intrusive rocks are poorly constrained, a prolonged magmatic activity is likely for these complex granitoid batholiths. *Zhou* and *Ren* (1994) reported hornblende Ar–Ar ages of 133.4 ± 0.4 Ma and 135.9 ± 0.5 Ma, respectively from the Tieshan quartz monzonite and Yangxin tonalite. Recent studies indicate that the granodiorite porphyry in Tongshankou stock and the diorite in Yangxin batholith yielded zircon SHRIMP U–Pb age of 140.6 ± 2.4 Ma (*Ma* et al., 2005) and 138.9 ± 2.8 Ma, respectively (*Li*, personal communication, 2005).

In southeastern Hubei numerous large Cu and Fe polymetallic deposits are associated with Late Mesozoic granitoid intrusions. They are hosted predominantly in sedimentrary rocks (i.e. Triassic carbonates, Ordovician to Permian limestone and marble, Silurian shale and sandstone) and to a lesser extent in the intrusive rocks (*Shu* et al., 1992; *Pan* and *Dong*, 1999). The main types of mineralisation are Fe, Cu, Cu–Fe, Fe–Cu and Cu–Au skarn deposits, which are spatially associated with granitoid batholiths (Fig. 2) and minor porphyry and stratabound Cu polymetallic deposits that are genetically related to granodiorite porphyry stocks, such as Tongshankou Cu–Mo porphyry and skarn, and Ruanjiawan W–Cu (Mo) skarn and stratabound deposits (Fig. 2).

Sampling and ore deposit geology

Eleven molybdenite samples were collected from five ore deposits: Fengshandong Cu- (Mo), Ruanjiawan W–Cu- (Mo), Qianjiawan Cu–Au, Tonglüshan Cu- (Fe) and Tongshankou Cu–Mo deposits. Re–Os ages for two of these samples were replicated. One phlogopite sample was collected from the Tieshan Fe- (Cu) deposit for Ar–Ar dating (Fig. 2).

The Fengshandong Cu- (Mo) deposit in the westernmost part of the Jiurui district (Fig. 1) is spatially associated with a small Late Jurassic to Cretaceous granodiorite porphyry stock (149–138 Ma, whole rock and biotite K–Ar). It has reserves of 0.4 million tonnes of Cu with ore grades of about 0.2–1 wt% Cu, as well as 50 thousand tonnes of Mo with an average grade of about 0.05 wt% Mo. The mineralisation comprising porphyry and skarn types is hosted in both the granodiorite porphyry and the Lower Triassic limestone and dolomite (Fig. 3a). The ore mineralogy includes chalcopyrite, pyrite, bornite, magnetite, chalcocite, molybdenite, with minor sphalerite and galena. Hydrothermal alteration is widespread, and consists of K-feldspar alteration, sercitization and skarn alteration. The ore is associated with the two latter alterations. Minor molybdenite occurs as fine-grained (0.2–1.1 mm) platelets in the porphyry Cu stockwork veins and is typically intergrown with chalcopyrite, pyrite and quartz. Sample FSD4 was collected from the porphyry Cu ores exposed on the surface.

The Ruanjiawan W–Cu- (Mo) deposit, located in the easternmost part of the Edong district (Fig. 1), is the only deposit enriched in tungsten with grades of 0.25–0.4 wt% W. The mineralisation is spatially associated with a small Late Mesozoic granodiorite porphyry body about 3 km south of the Yangxin batholith (Fig. 2). The mineralisation consists of skarn and stratabound ores, developed along the contact zone between the granodiorite stock and Ordovician carbonate rocks, as well as Silurian shales and sandstones (Fig. 3b). Ore minerals mainly include chalcopyrite, scheelite, pyrite, molybdenite, pyrrhotite, galena and sphalerite. Molybdenite occasionally occurs as fine-grained (0.2–0.5 mm) platelets in the skarn Cu orebodies, and is typically intergrown with chalcopyrite, pyrite, scheelite and diopside. Sample YJW4 was collected from skarn Cu ores exposed on the surface.

The Qianjiawan deposit is a recently discovered small skarn type Cu–Au deposit. It is located on the northern margin of the Yangxin batholith (Fig. 2) and is hosted by granodiorite and diorite, and Lower Triassic limestone and dolomite. The main ore minerals are chalcopyrite and pyrite. Minor disseminated

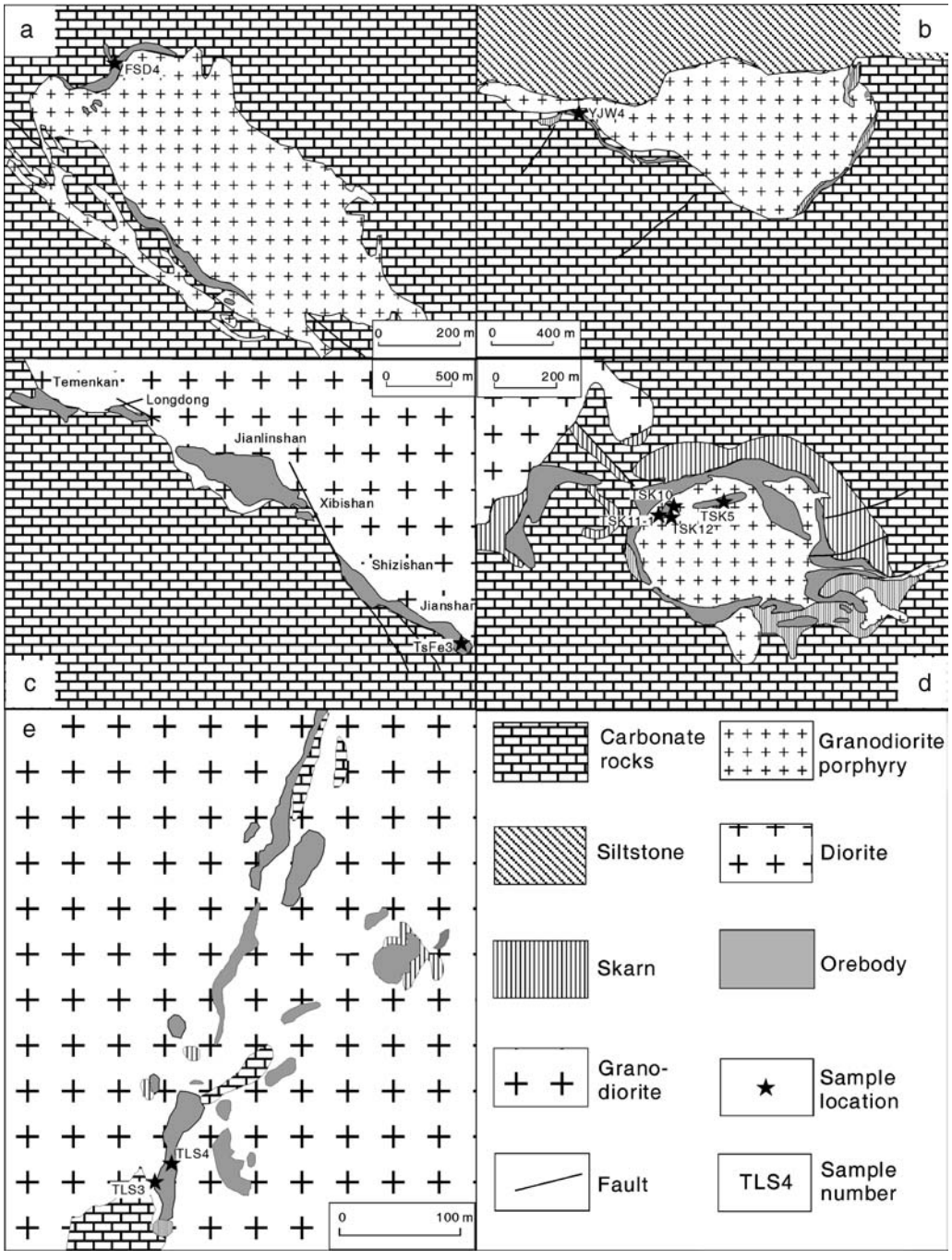

Fig. 3. Sketch maps of the (**a**) Fengshandong, (**b**) Ruanjiawan, (**c**) Tieshan, (**d**) Tongshankou, and (**e**) Tonglüshan deposits (modified from *Chang* et al., 1991; *Zhai* et al., 1992; *Shu* et al., 1992)

molybdenite occasionally occurs in small crystals (about 1.5 mm) in the Cu skarn. It is typically intergrown with chalcopyrite, pyrite and diopside. Sample QJW1 was collected from the skarn exposed on the surface.

The Tieshan deposit, a large skarn Fe- (Cu) deposit, located at the southern margin of the Tieshan batholith, has reserves of 160 million tonnes of Fe ore with an average grade of 52.1 wt% and 0.67 million tonnes of Cu ore with an average grade of 0.57 wt%. There are six major orebodies, i.e. Tiemenkan, Longdong, Jianlinshan, Xiangbishan, Shizishan and Jianshan, which are located at the contact between the diorite and the Triassic limestone (Fig. 3c). The individual orebodies are lenticular or podiform in shape, 360–870 m long and 10–80 m wide. Hydrothermal alteration assemblages include biotite, epidote, actinolite, carbonate, chlorite, phlogopite and kaolinite. These mineral phases commonly overprint early skarn and alkali feldspar alteration. The ore minerals are dominantly magnetite, hematite, siderite, pyrite, chalcopyrite and pyrrhotite. Common gangue minerals are phlogopite, garnet, diopside and wollastonite. Detailed studies showed that phlogopite occurs as aggregates of tabular crystals with a diameter of about 0.2–0.5 cm. It is typically intergrown with magnetite and diopside. Because of high $FeO + Fe_2O_3$ content (8.83–12.85 wt%), it is classified as Fe-bearing phlogopite (*Zhao* et al., 1990). Sample $TsFe_3$ was collected from massive magnetite skarn ores of the Jianshan orebody exposed on the surface.

The Tongshankou Cu–Mo porphyry deposit is located at the eastern margin of Lingxiang batholith (Fig. 2). It is genetically associated with a small Late Mesozoic granodiorite porphyry with an outcropping area of about 0.33 km^2 (Fig. 3d). It has reserves of 0.38 million tonnes of Cu ore with grade of about 0.3–3 wt% Cu, as well as an average grade of 0.047 wt% for Mo. The porphyry and skarn type mineralisation is hosted in the porphyry stock and in the surrounding Lower Triassic limestones and dolomites. Potassic feldspar, quartz–sericite (phyllic) and skarn alteration are well developed around the orebodies. There is a small Mo orebody in the northern part of granodiorite stock, where molybdenite occurs as tabular and flaky aggregates along the margins of the veins. Molybdenite ranges from 0.2 to 0.3 mm in size, and is commonly intergrown with chalcopyrite, pyrite, quartz and K-feldspar. Samples TSK5, TSK10 and TSK12 were collected from the quartz–sericite, and sample TSK11-1 from the potassic feldspar alteration zones.

The Tonglüshan deposit, at the northern margin of the Yangxin batholiths (Fig. 2), is the largest Cu- (Fe) skarn deposit in China. It has reserves of 1.1 million tonnes of Cu with an average grade of 1.78 wt% Cu and 5.7 million tonnes of Fe with an average grade of 41.1 wt% Fe. The mineralisation is spatially associated with the Yangxin granodiorite intrusion. This deposit consists of 12 individual orebodies trending NE 20° and is approximately 2100 m long and 600 m wide. The lenticular orebodies occur at the contact zones between the Yangxi batholith and Lower Triassic marbles and along roof pendants of carbonate rocks within the granodiorite (Fig. 3e). Hydrothermal alteration consists of skarn and its retrograde alteration comprising quartz, phlogopite, kaolinite and carbonates. The Cu–Fe mineralisation is associated with magnesian and calcic-magnesian skarns consisting of diopside, hessonite and phlogopite. The main ore minerals are chalcopyrite, bornite, pyrite, magnetite, molybdenite and sphalerite. In the southern part of the mine, there is a small Mo-rich orebody. Molybdenite occurs as fine-grained (0.2–1.0 mm) aggregates in both the skarn ores and granodiorite. It is typically inter-

grown with pyrite, chalcopyrite, garnet, diopside, feldspar, and quartz. Samples TLS3 and TLS4 were collected from the altered granodiorite and Mo-bearing skarn ore, respectively, and exhibit different mineral assemblage. The former includes feldspar, quartz, chalcopyrite, pyrite and molybdenite; the latter includes chlorite, garnet, calcite and molybdenite with minor pyrite.

Analytical methods

Re–Os dating

Eleven molybdenite samples were identified under an optical microscope and magnetically separated, and then fresh, non-oxidized molybdenite separates (0.2–0.5 mm) were handpicked under a binocular microscope. Re–Os isotope analyses were performed at the Re–Os Laboratory, National Research Center of Geoanalysis, Chinese Academy of Geological Sciences (NRCGCAGS). *Du* et al. (2004) have described the chemical separation procedure, which is summarized below in detail.

A Carius tube (a thick-walled borosilicate glass ampoule) digestion was used. The weighed sample was loaded in a Carius tube through a thin neck long funnel. The mixed ^{190}Os and ^{185}Re spike solutions and 4 ml of 10 mol/L HCl and 4 ml of 16 mol/L HNO_3 were loaded while the bottom part of the tube was frozen at -80 to $-50\,^{\circ}C$ in an ethanol-liquid nitrogen slush; the top was sealed using an oxygen-propane torch. The tube was then placed in a stainless-steel jacket and heated for 12 hours at 230 °C. Upon cooling, the bottom part of the tube was kept frozen. Then the neck of the tube was broken and the contents poured into a distillation flask. The residue was washed out with 40 ml of water.

Osmium was distilled twice. In the first distillation step, OsO_4 was distilled at 105–110 °C for 50 minutes and trapped in 10 ml of water. The residual Re-bearing solution was saved in a 150 ml beaker for Re separation. The water trap solution plus 40 ml of water was distilled a second time. The OsO_4 was distilled for 1 hour and trapped in 10 ml of water that was used for ICP-MS (TJA PQ ExCell) determination of the Os isotope ratio.

The Re-bearing solution was evaporated to dryness, and 1 ml of water was added twice while heating to near-dryness. Ten milliliter of 5 mol/L NaOH was added to the residue followed by Re extraction with 10 ml of acetone in a 120 ml Teflon separation funnel. The water phase was then discarded and the acetone phase washed with 2 ml of 5 mol/L NaOH. The acetone phase was transferred to a 150 ml Teflon beaker that contained 2 ml of water. After evaporation, the Re was dissolved in 1 ml of water that was used for the ICP-MS determination of the Re isotope ratio. Cation-exchange resin was used to remove Na if the salinity of the Re-bearing solution was more than 1 mg/ml (*Du* et al., 2004).

Average blanks for the total Carius tube procedure as described above were 11 ± 1 pg Re and 1.1 ± 0.3 pg Os. The analytical reliability was tested by repeated analyses of molybdenite standard HLP from a carbonatite vein-type Mo–Pb deposit in the Jinduicheng-Huanglongpu area of Shanxi Province, China. The average Re–Os age for HLP is 220.0 ± 2.6 Ma (95% confidence), and is consistent with the certified value of 221.4 ± 5.6 Ma (*Du* et al., 2004). The measured average

Re and Os concentrations for HLP are $282.7 \pm 0.22\,\mu g/g$ and $655.6 \pm 4.8\,ng/g$, respectively, in accordance with the certified values of $283.8 \pm 6.2\,\mu g/g$ and $659.0 \pm 14\,ng/g$ (*Du* et al., 2004). The decay constant used for ^{187}Re of 1.666×10^{-11}/year has an absolute uncertainty of ± 0.017 (1.0%) (*Smoliar* et al., 1996).

Ar–Ar dating

Fresh phlogopite (sample $TsFe_3$) was collected from the Tieshan Fe- (Cu) deposits. All measured samples were crushed and purified with a magnetic separator and then cleaned by ultrasonic treatment under ethanol. The purity of these mineral grains (0.08–0.15 mm) is more than 99%. Samples were wrapped in aluminum foil and loaded into a tube of Al foil, together with 2 or 3 monitor samples. The tubes were sealed into a quartz bottle (40 mm high; 50 mm in diameter). The bottle was irradiated for 51 h 46 min in a nuclear reactor (The Swimming Pool Reactor, Chinese Institute of Atomic Energy, Beijing). The reactor delivers a neutron flux of $\sim 6.0 \times 10^{12}\,n \cdot cm^{-2}\,s^{-1}$. The integrated neutron flux is about $1.16 \times 10^{18}\,n \cdot cm^{-2}$. After irradiation, the samples and monitors were removed from the quartz bottle and then loaded into the vacuum extraction system. They were baked out for 48 h at 120–150 °C. The Ar extraction system comprises an electron bombardment heated furnace in which the samples are heated under vacuum. A thermocouple was used to monitor and control the temperature of the furnace. The furnace can automatically attain the set temperature and maintain it within a range of few degrees. The released gases are admitted to a purification system. Heating-extraction for each temperature increment and purification lasted 30 min each. The purification system uses a U-tube cooled with a mixture of acetone and dry ice, a titanium sublimation pump at 38A filament current and a titanium sponge

Table 1. *Re–Os data of molybdenite from the Cu–Fe–Au–Mo- (W) ore deposits in southeastern Hubei, Middle–Lower Yangtze River metallogenic belt*

Deposits	Samples	Weight/(g)	Re/(μg/g)	^{187}Re/(μg/g)	^{187}Os/(ng/g)	Model age/(Ma)
Ruanjiawan	YJW4	0.01804	24.80 ± 0.20	15.59 ± 0.13	37.34 ± 0.28	143.6 ± 1.7
Fengshandong	FSD4	0.00151	436.5 ± 3.6	274.4 ± 2.2	659.2 ± 7.4	144.0 ± 2.1
Qijiawan	QJW1	0.00165	334.9 ± 2.7	210.5 ± 1.7	483.3 ± 4.3	137.7 ± 1.7
Tonglüshan	TLS3	0.00151	665.4 ± 5.2	418.2 ± 3.3	961.4 ± 8.0	137.8 ± 1.7
Tonglüshan	TLS4	0.00235	305.7 ± 2.5	192.1 ± 1.6	442.7 ± 4.0	138.1 ± 1.8
Tongshankou	TSK10	0.00303	203.6 ± 1.7	128.0 ± 1.1	306.3 ± 2.3	143.5 ± 1.7
Tongshankou	TSK5	0.00317	224.3 ± 1.7	141.0 ± 1.1	334.6 ± 3.1	142.3 ± 1.8
Tongshankou	TKS11-1	0.00313	178.3 ± 1.6	112.1 ± 1.0	266.0 ± 2.3	142.3 ± 2.0
Tongshankou	TKS11-1	0.02013	175.7 ± 1.4	110.4 ± 0.9	264.6 ± 2.0	143.7 ± 1.8
Tongshankou	TKS12	0.00315	232.3 ± 1.9	146.0 ± 1.2	347.7 ± 2.8	142.8 ± 1.9
Tongshankou	TKS12	0.02009	235.2 ± 1.8	147.8 ± 1.1	351.0 ± 2.8	142.4 ± 1.9

Note: Decay constant $\lambda(^{187}Re) = 1.666 \times 10^{-11}$/year (*Smoliar* et al., 1996). Uncertainties are absolute (2σ) including the uncertainties on Re and ^{187}Os concentrations and the ^{187}Re decay constant

furnace at 800 °C. Finally the gases were purified by two Sorb-AC pumps at room temperature. Purified Ar was trapped in an activated charcoal finger at liquid-nitrogen temperature, and then released into the MM-1200B Mass Spectrometer to analyze Ar isotopes.

Measured isotopic ratios were corrected for mass discrimination, atmospheric Ar component, blanks and irradiation induced mass interference. The correction factors of interfering isotopes produced during irradiation were determined by analysis of irradiated K_2SO_4 and CaF_4 pure salts and their values are: $(^{36}Ar/^{37}Ar)_{Ca} = 0.000240$, $(^{40}Ar/^{39}Ar)_K = 0.004782$, $(^{39}Ar/^{37}Ar)_{Ca} = 0.000806$. The blanks of the $m/e = 40$, 39, 37, 36 are less than 6×10^{-15}, 4×10^{-16}, 8×10^{-17} and 2×10^{-17} mol, respectively. The decay constant used is $\lambda = 5.543 \times 10^{-10}$ a^{-1} (*Steiger* and *Jäger*, 1977). All ^{37}Ar was corrected for radiogenic decay (half-life 35.1 days). The un-

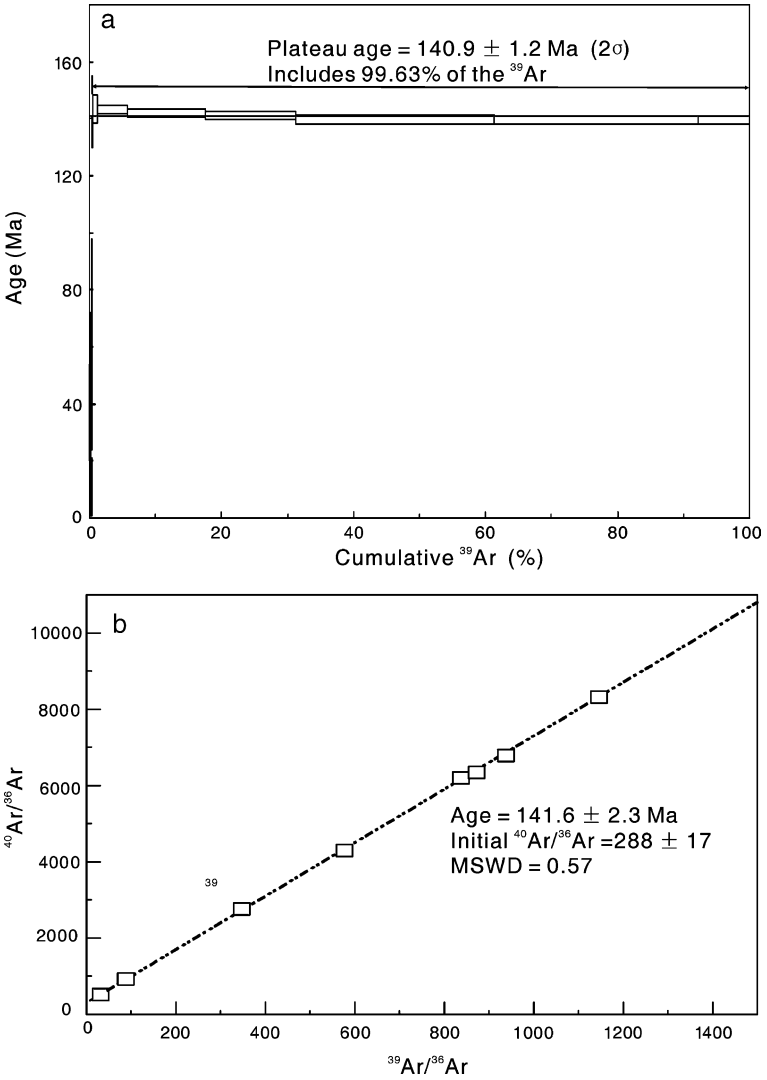

Fig. 4. Plateau and isochron Ar–Ar age of phlogopite from the Tienshan Fe- (Cu) skarn deposit

certainty for each apparent age is given at one standard deviation. The monitor used in this work is an internal standard: Fangshan biotite (ZBH-25) whose age is 132.7 ± 1.2 Ma and potassium content is $7.579 \pm 0.030\%$ (*Wang*, 1983). The $^{40}Ar/^{36}Ar$ vs. $^{39}Ar/^{36}Ar$ isochron diagram was defined by using the program ISOPLOT version 2.49 of *Ludwig* (2001).

Results

The Re–Os abundances and isotopic data for molybdenites are presented in Table 1. As shown in Table 1, the molybdenites from five investigated deposits yielded Re–Os model ages ranging from 137.7 ± 1.7 to 144.0 ± 2.1 Ma. Four molybdenites from the Tongshankou deposit yielded six ages from 142.3 ± 1.8 to 143.7 ± 1.8 Ma, with a mean value of 142.8 ± 1.9 Ma. Two molybdenites from the Tonglüshan deposit yielded 137.8 ± 1.7 Ma and 138.1 ± 1.8 Ma, with a mean value of 138.0 ± 1.8 Ma.

Twelve step-heating experiments at temperatures ranging from 500 to 1350 °C were performed for sample $TsFe_3$. The Ar–Ar age spectra of the analyzed samples are presented in Fig. 4a, and the results of the Ar–Ar data are summarized in Table 2. Plateau ages were determined using the criteria of *Dalrymple* and *Lamphere* (1971), specifying the presence of at least three continuous incremental heating steps with statistically indistinguishable ages and constituting about 65% of the total ^{39}Ar released during the experiment. The phlogopite $TsFe_3$ from Tieshan yielded a well-defined plateau age of 140.9 ± 1.2 Ma that encompassed 99.63 percent of the gas released (Fig. 4a and Table 2). A well-defined isochron age of 141.6 ± 2.3 Ma was calculated from ^{40}Ar and ^{39}Ar data. The initial value of 288 ± 17 is within the experimental uncertainty of the atmospheric argon value of 295.5 ± 5 (Fig. 4b).

Table 2. *Ar–Ar data for phlogopite sample $TsFe_3$ from the Tieshan Fe- (Cu) skarn deposit in southeastern Hubei, Middle–Lower Yangtze River metallogenic belt*

T (°C)	($^{40}Ar/^{39}Ar$)m	($^{36}Ar/^{39}Ar$)m	($^{37}Ar/^{39}Ar$)m	($^{38}Ar/^{39}Ar$)m	$^{39}ArK \times 10^{-12}$/mol	($^{40}Ar^*/^{39}Ar$)	^{39}ArK (%)	Apparent age (±1s Ma)
500	7.9297	0.0208	0.0486	0.0319	20.16	1.7859	0.17	37 ± 17
600	21.6221	0.0659	0.3372	0.0385	2.33	2.1672	0.02	45 ± 27
700	10.3361	0.0332	0.1092	0.0349	9.41	0.5273	0.08	11 ± 10
800	22.5987	0.0665	0.2858	0.0312	11.53	2.9654	0.1	61 ± 37
900	15.7047	0.0305	0.3019	0.0282	20.05	6.6959	0.16	135.4 ± 5.5
1000	10.4337	0.0113	0.0245	0.0181	68.94	7.1039	0.58	143.3 ± 5.0
1100	7.9526	0.0029	0.0043	0.0147	549.83	7.0975	4.62	143.2 ± 1.5
1150	7.4001	0.0012	0.0032	0.0141	1411.62	7.0428	11.87	142.1 ± 1.5
1200	7.2548	0.0009	0.0025	0.0143	1626.06	6.9925	13.66	141.2 ± 1.5
1250	7.2635	0.0011	0.0008	0.0141	3575.79	6.9204	30.06	139.8 ± 1.6
1300	7.2247	0.0011	0.001	0.0143	3669.59	6.9053	30.84	139.5 ± 1.6
1350	7.4247	0.0017	0.0019	0.0141	932.93	6.9085	7.84	139.5 ± 1.6

Note: Sample weight = 40.00 mg, J = 0.011639

Discussion

Significance of Re contents and Re–Os decoupling in molybdenite

As shown in Table 2, molybdenite from the Ruanjiawan W–Cu- (Mo) deposit has significantly lower Re contents than the other Cu–Fe–Mo–Au deposits studied. The former has low Re concentration (24.80 μg/g), the latter exhibit higher Re concentrations (175.7–665.4 μg/g). These higher values are similar to the Re contents in molybdenite from other porphyry and skarn Cu–Mo deposits worldwide (e.g. *Mao* et al., 1999, 2006a; *McCandless* and *Ruiz*, 1993; *Watanabe* and *Stein*, 2000; *Selby* and *Creaser*, 2001a, b; *Berzina* et al., 2005). *Mao* et al. (1999) suggested that the Re content in molybdenites could reflect the source of the deposit with Re content decreasing from mantle to I-type to S-type granite related deposits. *Stein* et al. (2001) also suggested that molybdenites from deposits with a mantle component have significantly higher Re contents than crustally derived ones. Low Re concentrations (<20 ppm) in molybdenite are highly diagnostic of a metamorphic derivation (*Stein*, 2006). This implies that the Ruanjianwan W–Cu-(Mo) deposit contains a higher crustal component than the other Cu–Mo–Fe–Au deposits studied.

It is to be noted that molybdenite from the same deposit can have variable Re contents (Table 1). In the Tonglüshan deposit molybdenite sample TLS3 (665.4 μg/g) has a significantly higher Re content than sample TLS4 (305.7 μg/g). In addition, there are differences in the total Re contents among molybdenites form the Tongshankou deposit. We assume that the Re content in molybdenite is related to the mineral assemblage.

Many studies indicate that there might be a decoupling effect in the Re–Os molybdenite system (e.g. *Kosler* et al., 2003; *Stein* et al., 2003). *Selby* and *Creaser* (2004) pointed out that overcoming this decoupling effect is of critical importance in obtaining accurate and reproducible Re–Os molybdenite dates. Fine grained (<2 mm) molybdenite appears to show little decoupling and therefore accurate Re–Os ages can be determined from small quantities of material of such samples (as little as 1 mg). In contrast, geologically old, and coarse-grained molybdenite samples may require as much as 40 mg of aliquot from a much larger mineral separate to overcome Re–Os decoupling effects (*Selby* and *Creaser*, 2004). Repeated Re–Os determinations of two molybdenite samples (TSK11-1 and TSK12) from the Tongshankou deposit were undertaken using about 3 and 20 mg sample aliquants of the same mineral separate (Table 1), and these analyses yielded reproducible Re–Os ages all within analytical uncertainty of each other. In addition, the molybdenite in this study is fine grained and has higher Re contents (Table 2). From this we conclude that decoupling effects in the Re–Os molybdenite system in the studied molybdenites are negligible, and that the data we obtained are reliable for the timing of molybdenites formation.

Timing of Cu–Fe–Au–Mo- (W) mineralisation

Compared with K–Ar and Ar–Ar ages, the Re–Os chronometer in molybdenite is remarkably robust, not easily being disturbed by younger hydrothermal, meta-

morphic and/or tectonic events (*Stein* et al., 1998, 2001). In general, the Re–Os ages of molybdenite are consistent with the SHRIMP zircon U–Pb ages of intrusion-related ore deposits (e.g. *Stein* et al., 1997; *Selby* and *Creaser*, 2001b; *Selby* et al., 2002). Therefore, Re–Os ages can directly record the timing of the primary sulfide mineralisation event (e.g. *Watanabe* and *Stein*, 2000; *Raith* and *Stein*, 2000; *Selby* and *Creaser*, 2001a, b; *Selby* et al., 2002). *Suzuki* et al. (1996) proposed that the Re–Os closure temperature for vein molybdenite is around 500 °C. Moreover, the Re–Os systematics in molybdentite is not affected by prolonged (~2–8 Ma) and high temperature (~400–500 °C) hydrothermal activity (*Selby* and *Creaser*, 2001a, b). Molybdenites from the Qianjiawan and Tonglüshan deposits, that are genetically associated with Yangxin granitic rocks, have Re–Os ages of 137.7 ± 1.8 Ma and 138.0 ± 1.7 Ma. These ages are slightly older than the hornblende Ar–Ar age (135.9 ± 0.5 Ma) of the Yangxin tonalite (*Zhou* and *Ren*, 1994), but are within the uncertainty of the zircon SHRIMP U–Pb age of 138.9 ± 2.8 Ma of the related granodiorite (*Li*, personal communication, 2005). In addition, the molybdenite Re–Os ages (142.3 ± 1.8 to 143.7 ± 1.8 Ma) of the Tongshankou deposit are also almost identical to the zircon SHRIMP U–Pb ages of 140.6 ± 2.4 Ma of the related granodiorite porphyry stock (*Ma* et al., 2005). Consequently, the Re–Os molybdenite ages reported in this study provide important information to constrain the absolute timing of Cu–Fe–Au–Mo- (W) mineralisation in the Middle–Lower Yangtze River metallogenic belt. The molybdenite Re–Os ages that were obtained are as follows: 144.0 ± 2.1 Ma for Fengshandong, 143.6 ± 1.7 Ma for Ruanjiawan, 137.7 ± 1.7 Ma for Qianjiawan, 142.8 ± 1.9 Ma for Tongshankou and 138.0 ± 1.8 Ma for Tonglüshan. As discussed above these ages represent the ages of ore formation.

It was demonstrated in many studies that Ar–Ar dating of phlogopite could be used to reliably date hydrothermal ore deposits (e.g. *Yu* and *Mao*, 2004; *Peng* et al., 2006). As seen in Table 2, there are four apparent ages in the low temperature intervals (500–800 °C) in sample $TsFe_3$ from the Tieshan deposit. However, the Ar release of those stages only reaches 0.37%. Hence, the small fluctuations of apparent ages seen in the Ar–Ar stepwise heating stage spectra (Fig. 4a) are probably due to initial loss of small quantities of argon from the edges of mineral grains. Ar–Ar stepwise heating analyses of phlogopite in the higher temperature intervals yielded uniform and remarkably flat Ar–Ar age spectra with a plateau age of 99.63% of the total ^{39}Ar released (Fig. 4a), indicating the absence of excess Ar or any diffusive Ar loss. Thus, the well-defined Ar–Ar plateau age of 140.9 ± 1.2 Ma is considered to be a reliable estimate for the crystallisation time of phlogopite.

Fluid inclusion studies by *Chang* et al. (1991) showed that the minimum formation temperature of Fe mineralisation in the Tieshan deposit ranged from 420 to 545 °C. Calculations and experimental diffusion studies indicate that the closing temperature of the Ar–Ar system in phlogopites is between 400 and 510 °C (*Giletti* and *Tullis*, 1977). Based on these considerations, we concluded that the Ar–Ar system in phlogopite remained to be closed with ore deposition in the Tieshan deposit. Phlogopite from the Tieshan deposit, that is spatially and genetically associated with diorite, rather than quartz monzonite (*Chang* et al., 1991), has Ar–Ar age of 140.9 ± 1.2 Ma. The age is slightly older than the hornblende Ar–Ar age

(133.4 ± 0.4 Ma) of the quartz monzonite (*Zhou* and *Ren*, 1994), but we assume that the phlogopite Ar–Ar age in this study constrains the formation of the Tieshan skarn Fe- (Cu) deposit at 140.9 ± 1.2 Ma, coincident with the other porphyry, skarn and stratabound Cu–Fe–Au–Mo- (W) deposits in southeastern Hubei, China.

Implications for regional metallogeny

As shown in Fig. 1, Late Mesozoic porphyry, skarn and stratabound Cu–Fe–Au–Mo- (W) deposits are present in the Middle–Lower Yangtze River metallogenic belt, whereas magnetite-rich porphyry deposits developed in the Ningwu Cretaceous volcanic–sedimentary basin. Albite from the Meishan and Taocun, two of the magnetite porphyry deposits, yielded Ar–Ar plateau ages of 122.90 ± 0.16 Ma and 124.89 ± 0.30 Ma, and phlogopite from the Zhongshan-Gushan ore field gave a plateau age of 126.7 ± 0.17 Ma (*Yu* and *Mao*, 2004). These precise molybdenite Re–Os and mica Ar–Ar ages show that the porphyry, skarn and stratabound Cu–Fe–Au–Mo deposits were earlier and formed, between 135.5 and 144.9 Ma (Table 3). As shown in Table 3, an important regional metallogenic event occurred in the Late Jurassic to Early Cretaceous in the Middle–Lower Yangtze River belt, where the Edong Fe–Cu (Au) was formed between 137.7 and 143.6 Ma, Jiurui Cu–Au (Mo) between 137.0 and 144.0 Ma, Anqing Cu–Fe–Mo (Au) 138.0 and 141.6 Ma and Tongling Cu–Au 135.5 and 144.9 Ma (Table 3).

Late Jurassic to Early Cretaceous mineralisation is not only widespread in the Middle–Lower Yangtze River belt. Many porphyry and skarn Mo deposits at the southern and northern margin of North China Block also formed between 131.6 and 145.8 Ma and 134 and 148 Ma, respectively (*Stein* et al., 1997; *Mao* et al., 2005). Regional granite related W–Sn mineralisation occurred at 140–126 Ma in South China (*Mao* et al., 2006b). Moreover, regional mineralisation in the Middle–Lower Yangtze River belt is similar to that seen in the Lachlan Fold Belt (440 Ma) (*Vos* et al., 2005), and in southwestern North America (74–70 Ma, 60–55 Ma) (*McCandless* and *Ruiz*, 1993). *Vos* et al. (2005) proposed that rapid changes in subduction dynamics, such as slab break-off, may have played a crucial role in the formation of giant metallic ore provinces. Following this concept, we speculate that regional-scale mineralisation processes in the Middle–Lower Yangtze River belt possibly were caused by similar geodynamic processes.

Zhai et al. (1996) suggested that the deposits of the Middle–Lower Yangtze River metallogenic belt formed in an aborted continental rift setting. Recently, *Wang* et al. (2003) proposed that most of the Late Mesozoic intrusive rocks that are associated with Cu–Fe–Au–Mo mineralisation in the Middle–Lower Yangtze River metallogeinc belt are of adakitic affinity. From the geochemical signature of these rocks, it is suggested that lower crustal delamination and lithospheric thinning took place during the Late Mesozoic in East China, accompanied by the emplacement of the adakitic magma (*Xu* et al., 2002). Such adakitic magmas, derived from melting of the delaminated lower crust, were favorable for the formation of porphyry Cu–Mo deposits in this area (*Wang* et al., 2004). In addition, geochemical characteristics of Cretaceous volcanic rocks also suggest that asthenospheric upwelling and lithospheric thinning occurred in this area (*Wang* et al., 2001). Regional-scale mineralising processes took place during the Late Mesozoic,

Table 3. *Re–Os molybdenite and Ar–Ar ages of some Cu–Fe–Au–Mo deposits in the Middle–Lower Yangtze River metallogenic belt*

Ore districts	Deposits	Samples	Age (Ma)	Analytical method and comments	Reference
Edong	Tieshan	phlogopite in massive skarn ore	140.9 ± 1.2	Ar–Ar plateau age, isochron age is 141.6 ± 2.3 Ma	This study
	Tongshankou	Molybdenite in the phyllic alteration zone	142.9 ± 1.7	Average of two Re–Os model ages ranging from 143.5 ± 1.73 to 142.3 ± 1.79 Ma	This study
	Tonglüshan	Molybdenite in skarn ore	138.0 ± 1.7	Average of two Re–Os model ages ranging from 137.8 ± 1.67 to 138.1 ± 1.75 Ma	This study
	Qianjiawan	Molybdenite in skarn ore	137.7 ± 1.7	Re–Os model age	This study
	Ruanjiawan	Molybdenite in granodiorite	143.6 ± 1.7	Re–Os model age	This study
Jiurui	Fengshandong	Molybdenite in granodiorite	144.0 ± 2.1	Re–Os model age	This study
	Chengmengshan	Molybdenite in quartz vein	141.0 ± 3.0	Isochron dating of five Re–Os model ages ranging from 139.3 to 144.2 Ma	*Wu* and *Zou* (1997)
		Molybdenite in quartz porphyry rock	137.0 ± 2.3	Isochron dating of six Re–Os model ages range from 136.4 to 144.0 Ma	*Wu* and *Zou* (1997)
		Molybdenite in Mo ore body	142.3 ± 2.3	Re–Os model age	*Mao* et al. (2006a)
Anqing	Anqing	Molybdenite in veinlet ore	138.4 ± 2.0	Average of five Re–Os model ages ranging from 134.7 ± 2.3 to 142.6 ± 1.7 Ma	*Mao* et al. (2006a)
	Tukuangli	Molybdenite	141.6 ± 1.9	Average of five Re–Os model ages ranging from 139.4 ± 2.2 to 143.7 ± 1.6 Ma	*Mao* et al. (2006a)
	Yueshan	Molybdenite in the no. 1 orebody	138.0 ± 2.5	Os–Os model age	*Sun* et al. (2003)

(*continued*)

Table 3 (*continued*)

Ore districts	Deposits	Samples	Age (Ma)	Analytical method and comments	Reference
Tongling	Shatanjiao	Molybdenite	140.3 ± 1.8	Average of six Re–Os model ages ranging from 136.9 ± 2.2 to 142.8 ± 1.6 Ma	*Mao* et al. (2006a)
	Nanyangshan	Molybdenite	139.3 ± 1.3	Average of seven Re–Os model ages ranging from 136.9 ± 2.1 to 141.1 ± 0.5 Ma	*Mao* et al. (2006a)
	Datuanshan	Molybdenite in the no. 2 Mo orebody	139.1 ± 2.7	Isochron dating of six Re–Os model ages ranging from 138.0 ± 3.2 Ma to 140.8 ± 2.0 Ma	*Mao* et al. (2006a)
	Longhushan	Molybdenite in diorite	139.0 ± 0.3	Re–Os model age, the Os–Os model age is 138.1 ± 2.5 Ma	*Sun* et al. (2003)
	Jingkouling	Molybdenite in skarn ore	137.0 ± 0.2	Isochron age of six Re–Os model ages ranging from 136.8 Ma to 137.4 Ma	*Meng* et al. (2004)
	Tongguanshan	Fuchsite associated with chalocopyrite	135.5 ± 0.5	Ar–Ar plateau age, isochron age is 137.7 ± 2.8 Ma	*Meng* et al. (2004)
	Laomiaojishan	Fuchsite associated with chalocopyrite	144.9 ± 0.4	Ar–Ar plateau age, isochron age is 150.3 ± 3.0 Ma	*Meng* et al. (2004)
	Talimu	Molybdenite in altered granodiorite	138.6 ± 0.2	Re–Os model age	*Zeng* et al. (2004)
	Qingyang	Molybdenite in skarn and quartz vein ore	137.3 ± 2.5	Average of two Os–Os model ages ranging from 136.4 ± 2.5 Ma to 138.1 ± 2.5Ma	*Sun* et al. (2003)

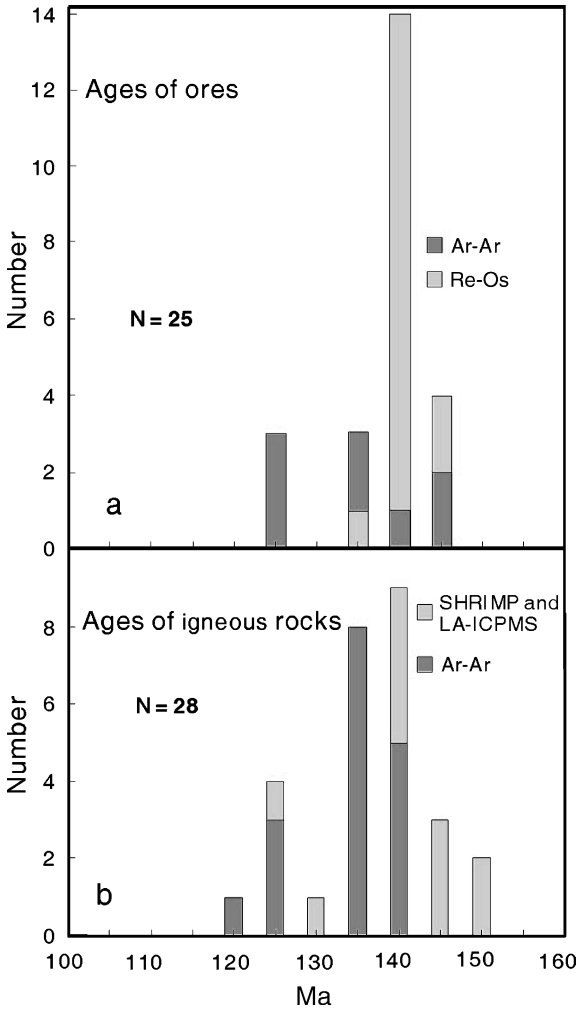

Fig. 5. Histograms of isotope ages for (**a**) Cu–Fe–Au–Mo- (W) deposits and (**b**) Igneous rocks in the Middle–Lower Yangtze River metallogenic belt. Data (**a**) from *Wu* and *Zou* (1997), *Sun* et al. (2003), *Zeng* et al. (2004), *Meng* et al. (2004); and *Mao* et al. (2006a, b, this study). Data (**b**) from *Cheng* et al. (1985), *Zhou* and *Ren* (1994), *Wu* et al. (1996), *Zhang* et al. (2003), *Zang* (2004), *Wang* et al. (2004a–c), *Xu* et al. (2004), *Xie* et al. (2006), and *Ding* et al. (2006)

with two pluses occurring at ∼140 and ∼125 Ma (Fig. 5), coincident with voluminous igneous rocks in the Middle–Lower Yangtze River metallogenic belt. Consequently, rock- and ore-forming processes may have occurred during the same tectono-magmatic episode in this area. Mineralising pulses and associated magmatism and the geodynamic framework, suggest that the Late Jurassic to Early Cretaceous Cu–Fe–Au–Mo mineralisation in the Middle–Lower Yangtze River metallogenic belt is associated with an extensional regime, which was probably the result of lower crustal delamination and lithospheric thinning, a scenario that is also supported by deep seismic reflection profiling (*Lü* et al., 2005).

Conclusions

Re–Os molybdenite and Ar–Ar phlogopite dating of Cu–Fe–Au–Mo- (W) deposits in southeastern Hubei, allow us to draw the following conclusions:

1. Decoupling effects in the Re–Os molybdenite system in the studied molybdenites are negligible; with molybdenite Re–Os ages of 144.0 ± 2.1 Ma for

the Fengshandong deposit, 143.6 ± 1.7 Ma for Ruanjiawan, 137.7 ± 1.7 Ma for Qianjiawan, 142.8 ± 1.9 Ma for Tongshankou and 138.0 ± 1.8 Ma for Tonglüshan; these ages are considered to represent the time of ore formation.
2. The phlogopite Ar–Ar age constrains the formation of the Tieshan skarn Fe-(Cu) deposit at 140.9 ± 1.2 Ma, coincident with the other porphyry, skarn and stratabound Cu–Fe–Au–Mo- (W) deposits in southeastern Hubei, China.
3. These data and the other published ages indicate that major Cu–Fe–Au–Mo-(W) metallogenic event occurred between Late Jurassic and Early Cretaceous in the Middle–Lower Yangtze River metallogenic belt, which is associated with lithospheric extension due to lower crustal delamination and lithospheric thinning.

Acknowledgements

We thank Zhang Zusong, Wei Shikun, Xiong Jizhuan, Li Xiangzhou, Yang Minyin and Zhou Shaodong for their kind help during the field investigations. Determination of molybdenite Re–Os isotopic compositions done by Ceng Fagang from National Research Center of Geoanalysis is greatly appreciated. We thank Professor Li Jianwei and Yan Danping for discussions, Editor J. G. Raith, D. Selby and J. Kosler for constructive comments that helped to greatly improve this manuscript. This work was supported jointly by National Science Foundation of China (40434011 and 40402011), State Key Laboratory of Geological Processes and Mineral Resources, China University of Geosciences (GPM40504), China Postdoctoral Science Foundation and State Key Laboratory of Ore Deposit Geochemistry, Institute of Geochemistry, Chinese Academy of Sciences China (200402). Franco Pirajno publishes with the permission of the Director of the Geological Survey of Western Australia.

References

Berzina AN, Sotnikov VI, Economou-Eliopoulos M, Eliopoulos DG (2005) Distribution of rhenium in molybdenite from porphyry Cu–Mo and Mo–Cu deposits of Russia (Siberia) and Mongolia. Ore Geol Rev 26: 91–113

Chang YF, Liu XP, Wu CY (1991) The copper-iron belt of the Lower and Middle Reaches of the Changjiang River. Geological Publishing House, Beijing (in Chinese with English abstract)

Chen J-F, Yan J, Xie Z, Xu X, Xing F (2001) Nd and Sr isotopic compositions of igneous rocks from the Lower Yangtze region in eastern China: constraints on sources. Phys Chem Earth (A) 26: 719–731

Cheng JF, Foland KA, Zhou TX (1985) The significance of granite gneisses in the lithosphere. In: *Wu Liren* et al. (ed) Theophrastus Publications, Athens, pp 217–237

Dalrymple GB, Lamphere MA (1971) $^{40}Ar/^{39}Ar$ technique of K–Ar dating: a comparison with the conventional technique. Earth Planet Sci Lett 12: 300–308

Ding X, Jiang S-Y, Zhao K-D, Nakumura E, Kobayashi K, Ni P, Gu L-X, Jiang Y-H (2006) In situ U–Pb SIMS dating and trace element (EMPA) composition of zircon from a granodiorite porphyry in the Wushan copper deposit, China. Mineral Petrol 86: 29–44

Du A-D, Wu SQ, Sun DZ, Wang SX, Qu WJ, Markey R, Stein H, Morgan J, Malinovskiy D (2004) Preparation and certification of Re–Os dating reference materials: Molybdenite HLP and JDC. Geostandard Geoanalyt Res 28: 41–52

Giletti BJ, Tullis J (1977) Studies in diffusion: pressure dependence of Ar diffusion in phlogopite mica. Earth Planet Sci Lett 35: 180–183

Kosler J, Simonetti A, Sylvester PJ, Cox RA, Tubrett MN, Wilton DHC (2003) Laser-ablation ICP-MS measurements of Re/Os in molybdenite and implications for Re–Os geochronology. Can Mineral 41: 307–320

Lü QT, Hou ZQ, Yang ZS, Shi DN (2005) Underplating and dynamic evolution model in the lower Yangtze area: constraints from geophysical data. Science in China (D) 34: 783–794

Ludwig K (2001) Isoplot/Ex, version 2.49: a geochrological toolkit for Microsoft Excel. Geochronology Center, Berkeley, Special Publication

Ma CQ, Li JW, Xu HJ, Zhang C (2005) Late Mesozoic large igneous rocks: magma underplating and inplating. Petrology and Geodynamics Conference Abstracts in China. pp 138–139 (in Chinese)

Mao J-W, Zhang Z, Zhang Z, Du A-D (1999) Re–Os isotopic dating of molybdenites in the Xiaoliugou W- (Mo) deposit in the northern Qilian Mountains and its geological significance. Geochim Cosmochim Acta 63: 1815–1818

Mao J-W, Xie G-Q, Zhang ZH, Li XF, Wang YT, Zhang CQ, Li YF (2005) Mesozoic large-scale metallogenic pluses in North China and corresponding geodynamics setting. Acta Petrologica Sinica 21: 169–188 (in Chinese with English abstract)

Mao J-W, Wang YT, Lehmann B, Yu JJ, Du A-D, Mei YX, Li YF, Zang WS, Stein HJ, Zhou TF (2006a) Molybdenite Re–Os and albite $^{40}Ar/^{39}Ar$ dating of Cu–Au–Mo and magnetite porphyry systems in the Yangtze River valley and metallogenic implications. Ore Geol Rev 29: 307–324

Mao J-W, Xie G-Q, Li XF, Zhang CQ, Wang YT (2006b) Mesozoic large-scale mineralisation and multiple lithospheric extensions in South China. Acta Geologica Sinica (English Edition) 80: 420–431

McCandless TE, Ruiz J (1993) Rhenium-osmium evidence for regional mineralisation in Southwestern North America. Science 261: 1282–1286

Meng YF, Yang ZS, Zeng PS, Xu WY, Wang XC (2004) Tentative temporal constraints of ore-forming fluid systems in Tongling metallogenic province. Mineral Deposits 23: 271–280 (in Chinese with English abstract)

Ningwu Research Group (1978) Porphyry iron deposits in Ningwu area. Geological Publishing House, Beijing (in Chinese)

Pan Y, Dong P (1999) The Lower Changjiang (Yangzi/Yangtze River) metallogenic belt, east China: intrusion- and wall rock-hosted Cu–Fe–Au, Mo, Zn, Pb, Ag deposits. Ore Geol Rev 15: 177–242

Pei RF, Hong DW (1995) The granites of South China and their metallogeny. Episodes 18: 77–86

Peng JT, Zhou M-F, Hu RZ, Shen NP, Yuan SD, Bi XW, Du A-D, Qu WJ (2006) Precise molybdenite Re–Os and mica Ar–Ar dating of the Mesozoic Yaogangxian tungsten deposit, Central Nanling District, South China. Mineral Deposita 41: 661–669

Raith JG, Stein HJ (2000) Re–Os dating and sulfur isotope composition of molybdenite from tungsten deposits in western Namaqualand, South Africa: implications for ore genesis and the timing of metamorphism. Mineral Deposita 35: 741–753

Selby D, Creaser RA (2001a) Re–Os geochronology and systematics in molybdenite from the Endako porphyry molybdenum deposit, British Columbia, Canada. Econ Geol 96: 197–204

Selby D, Creaser RA (2001b) Late and Middle Cretaceous mineralisation in the Northern Canadian Cordillera: constraints from Re–Os molybdenite dates. Econ Geol 96: 1461–1467

Selby D, Creaser RA, Hart CJ, Rombach CS, Thompson JFH, Smith MT, Bakke AA, Goldfarb RJ (2002) Absolute timing of sulfide and gold mineralisation: a comparison

of Re–Os molybdenite and Ar–Ar mica methods from the Tintina Gold Belt, Alaska. Geology 30: 791–794

Selby D, Creaser RA (2004) Macroscale NTIMS and microscale LA-MC-ICP-MS Re–Os isotopic analysis of molybdenite: testing spatial restrictions for reliable Re–Os age determinations, and implications for the decoupling of Re and Os within molybdenite. Geochim Cosmochim Acta 68: 3897–3908

Shu QA, Chen PL, Cheng JR (1992) Geology of iron–copper deposits in Eastern Hubei Province, China. Ministry of Metallurgical Industry Publishing House, Beijing (in Chinese)

Smoliar MI, Walker RJ, Morgan JW (1996) Re–Os ages of group IIA, IIIA, IVA and VIB iron meteorites. Science 271: 1099–1102

Steiger RH, Jäger E (1977) Subcommission on geochronology: convention on the use of decay constants in geo- and cosmochronology. Earth Planet Sci Lett 36: 359–362

Stein H, Scherstén A, Hannah J, Markey R (2003) Subgrain-scale decoupling of Re and ^{187}Os and assessment of laser ablation ICP-MS spot dating in molybdenite. Geochim Cosmochim Acta 67: 3673–3686

Stein HJ (2006) Low-rhenium molybdenite by metamorphism in northern Sweden: Recognition, genesis, and global implications. Lithos 87: 300–327

Stein HJ, Markey RJ, Morgan JW, Du A-D, Shu Y (1997) Precise and accurate Re–Os ages for molybdenite from the East Qinling molybdenum belt, Shanxi Province, China. Econ Geol 92: 827–835

Stein HJ, Sundblad K, Markey R, Motuza G (1998) Re–Os ages for Archean molybdenite and pyrite, Kuittila-Kiviso, Finland and Proterozoic molybdenite, Kabeliai, Lithuania: testing the chronometer in a metamorphic and metasomatic setting. Mineral Deposita 33: 329–345

Stein HJ, Markey RJ, Morgan JW, Hannah JL, Scherstén A (2001) The remarkable Re–Os chronometer in molybdenite: how and why it works. Terra Nova 13: 479–486

Sun W, Xie Z, Chen J, Zhang X, Chai Z, Du A, Zhao J, Zhang C, Zhou T (2003) Os–Os dating of copper and molybdenum deposits along the Middle and Lower reaches of the Yangtze River, China. Econ Geol 98: 175–180

Suzuki K, Shimizu H, Masuda A (1996) Re–Os dating of molybdenites from ore deposits in Japan: implication for the closure temperature of the Re–Os system for molybdenite and the cooling history of molybdenum ore deposits. Geochim Cosmochim Acta 60: 3151–3159

Vos IMA, Bierlein FP, Heithersay PS, Lister GS (2005) Geodynamic controls on giant metallogenic provinces: insights from gold provinces in southeast Australia. In: *Mao J-W, Bierlein FP* (eds) Mineral Deposit Research: Meeting the Global Challenge. Springer, pp 61–64

Wang Q, Zhao ZH, Xu JF, Li XH, Bao ZW, Xiong XL, Liu YM (2003) Petrogenesis and metallogenesis of the Yanshanian adakite-like rocks in the Eastern Yangtze Block. Science in China (D) 46 (Suppl): 164–176

Wang Q, Zhao ZH, Bao ZW, Xu JF, Liu W, Li CF, Bai ZH, Xiong XL (2004) Geochemistry and petrogenesis of the Tongshankou and Yinzu adakitic intrusive rocks and the associated porphyry copper-molybdenum mineralisation in southeast Hubei, East China. Resource Geology 54: 137–152

Wang SS (1983) Dating of the Chinese K–Ar standard sample (Fangshan biotite, ZBH-25) by using the ^{40}Ar/^{39}Ar method. Scientia Geologica Sinica 4: 315–321 (in Chinese with English abstract)

Wang Y, Liu D, Meny YF, Zheng P, Yang Z, Tian S (2004) SHRIMP U–Pb geochronology of the Xinqiao Cu–S–Fe–Au deposit in the Tongling ore district, Anhui. Geology in China 31: 169–173 (in Chinese with English abstract)

Wang Y, Liu D, Zheng P, Yang Z, Tian S (2004) SHRIMP U–Pb geochronology of pyroxene diorite in the Chaoshan gold deposit and its geological significance. Acta Geoscientica Sinica 31: 169–173 (in Chinese with English abstract)

Wang Y, Liu D, Zeng P, Yang Z, Meng Y, Tian S (2004) SHRIMP U–Pb geochronology of Xiaotonggunashan quartz-dioritic intrusions in Tongling district and its petrogenetic implication. Acta Petrologica et Mineralogica 23: 298–304 (in Chinese with English abstract)

Wang YL, Zhang Q, Wang Y (2001) Geochemical characteristics of volcanic rocks from Ningwu area, and its significance. Acta Petrologica Sinica 17: 565–575 (in Chinese with English abstract)

Watanabe Y, Stein HJ (2000) Re–Os ages for the Erdenet and Tsagaan Suvarga porphyry Cu–Mo deposits, Mongolia, and tectonic implications. Econ Geol 95: 1537–1542

Wu CL, Zhou XR, Huang XC, Zhang CH, Huang WM (1996) $^{40}Ar/^{39}Ar$ chronology of intrusive rocks from Tongling. Acta Petrologica et Mineralogica 15: 299–307 (in Chinese with English abstract)

Wu LS, Zou XQ (1997) Re–Os isotopic age study on the Chengmenshan Cu deposit in Jiangxi Province. Mineral Deposits 16: 376–381 (in Chinese with English abstract)

Xie G-Q, Mao J-W, Zhao CS (2005) Mineralizing pulses and geodynamic setting of Cu–Fe–Au polymetallic deposits in the Lower Yangtze valley, east-central China. In: *Mao J-W, Bierlein FP* (eds) Mineral Deposit Research: Meeting the Global Challenge. Springer, Berlin Heidelberg New York, pp 1201–1204

Xie G-Q, Mao J-W, Zhou SD, Ye HS, Yan QR, Zhang ZS (2006) SHRIMP zircon U–Pb dating for volcanic rocks of the Dasi Formation in southeast Hubei Province, middle-lower reaches of the Yangtze River and its implications. Chinese Science Bulletin 51: 3000–3009

Xu JF, Shinjo R, Defant MJ, Wang Q, Rapp RP (2002) Origin of Mesozoic adakitic intrusive rocks in the Ningzhen area of east China: partial melting of delaminated lower continental crust? Geology 30: 1111–1114

Xu X, Fan Q, O'Reilly SY, Jiang S, Griffin WL, Wang RC, Qiu JS (2004) U–Pb dating of zircons from quartz diorite and its enclaves at Tongguanshan in Anhui and its petrogenetic implication. Chinese Science Bulletin 49: 2073–2082

Yu JJ, Mao J-W (2004) $^{40}Ar–^{39}Ar$ dating of albite and phlogopite from porphyry iron deposits in the Ningwu basins in east-central China and its significance. Acta Geologica Sinica (English Edition) 78: 435–442

Zang WS (2004) Research on chronology of intrusive rocks and related tectonic-laying mineralisation in Tongling cluster. Beijing: Ph.D. Thesis of China University of Geosciences (in Chinese with English abstract)

Zeng PS, Yang ZS, Meng YF, Pei RF, Wang YB, Wang XC (2004) Temporal-spatial configuration and mineralisation of Yanshanian magmatic fluid systems in Tongling ore concentration area. Anhui province. Mineral Deposits 23: 298–309 (in Chinese with English abstract)

Zhai YS, Yao SZ, Lin XD, Zhou XN, Wan TF, Jin FQ, Zhou ZG (1992) Fe–Cu (Au) metallogeny of the Middle–Lower Changjiang region. Geological Publishing House, Beijing (in Chinese)

Zhai YS, Xiong YY, Yao SZ, Liu XD (1996) Metallogeny of copper and iron deposits in the Eastern Yangtze Carton, east-central China. Ore Geol Rev 11: 229–248

Zhang Q, Jian P, Liu DY, Wang YL, Qian Q, Wang Y, Xue H (2003) SHRIMP dating of volcanic rocks from Ningwu area and its geological implications. Science in China (D) 46: 830–837

Zhao YM, Lin WW, Bi CS, Li DX, Jiang CJ (1990) Skarn deposits of China. Geological Publishing House, Beijing (in Chinese with English abstract)

Zhou XR, Ren J (1994) Mesozoic granites in the Middle-Lower reaches of Yangtze River. Geological Publishing House, Beijing (in Chinese with English abstracts)

Authors' addresses: *G.-Q. Xie* (corresponding author; e-mail: guiqingxie@sohu.com), Institute of Mineral Resources, Chinese Academy of Geological Sciences, No. 26 Baiwanzhuang Road, Beijing 100037, China; *J.-W. Mao* (e-mail: jingwenmao@263.net), Institute of Mineral Resources, Chinese Academy of Geological Sciences, No. 26 Baiwanzhuang Road, Beijing 100037, China; *R.-L. Li* (e-mail: lrling@sohu.com), Development of Geological Center, China Geological Survey, No. 45 Fuwai Street, Beijing 100037, China; *W.-J. Qü* (e-mail: quwenjun03@163.com), National Research Centers of Geoanalysis, Chinese Academy of Geological Sciences, No. 26 Baiwanzhuang Road, Beijing 100037, China; *F. Pirajno* (e-mail: franco.pirajno@doir.wa.gov.au), Geological Survey of Western Australia, 100 Plain Street, Perth, WA 6004, Australia; *A.-D. Du* (e-mail: andaodu@163.com), National Research Centers of Geoanalysis, Chinese Academy of Geological Sciences, No. 26 Baiwanzhuang Road, Beijing 100037, China